IEEE Photonics Journal
An IEEE Photonics Society Publication

Open Access

# Plasmonic Near-Field Enhancement for Planar Ultra-Thin Photovoltaics

Volume 5, Number 5, October 2013

**Zhu Wang**
**Thomas P. White**
**Kylie R. Catchpole**

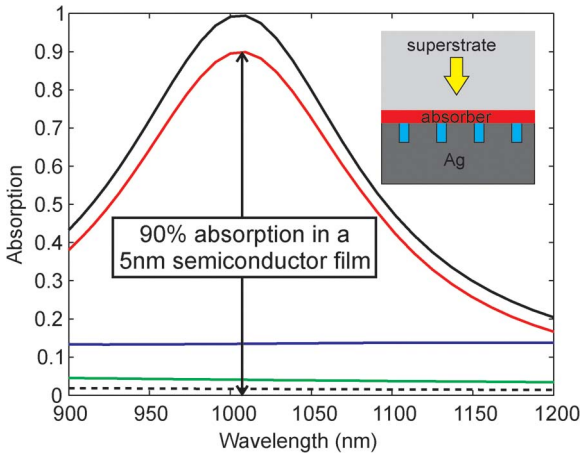


DOI: 10.1109/JPHOT.2013.2280518
1943-0655 

IEEE photonics SOCIETY

IEEE

# Plasmonic Near-Field Enhancement for Planar Ultra-Thin Photovoltaics

**Zhu Wang, Thomas P. White, and Kylie R. Catchpole**

Centre for Sustainable Energy Systems, Research School of Engineering, Australian National University, Canberra ACT 2600, Australia

*DOI: 10.1109/JPHOT.2013.2280518*


Manuscript received June 16, 2013; revised August 11, 2013; accepted August 16, 2013. Date of publication September 4, 2013; date of current version September 9, 2013. This work was supported by the Australian Research Council under Grants DP0880017 and DP130101009. Corresponding author: Z. Wang (e-mail: zhu.wang@anu.edu.au).

**Abstract:** We propose a planar ultrathin absorber concept exploiting plasmonic resonance absorption enhancement. We calculate a maximum absorption of 89.8% for TM-polarized normally incident light in a 5-nm thin-film absorber with a single-pass absorption of only 1.7%, i.e., a 53 times increase in absorption. Broadband and wide-angle absorption is demonstrated. Averaging over isotropic incidence for TM polarization, the absorption is enhanced by a factor of 48. Despite low TE absorption, the average absorption enhancement over all angles and both polarizations is 28, well above the 2-D Lambertian light-trapping limit of $\pi\ n$.

**Index Terms:** Grating, near-field, photovoltaic, plasmonic, solar cell.

## 1. Introduction

Thin-film solar cells are considered to be an effective route to cut the price of power generated from photovoltaics [1]. While current thin-film modules are based largely on amorphous Si, CdTe, and CIGS technology, there is growing interest in alternative strongly absorbing and earth-abundant inorganic semiconductors, which may offer low extraction costs and global-scale capacity [2]. The electrical properties of many such materials are poor, and electrons and holes can only travel several tens of nanometers before recombination. Therefore, to increase energy conversion efficiency, the absorbing layer thickness has to be on the order of nanometers so that the photocarriers (electron-hole pairs) can be fully collected. In such thin layers, light absorption is normally low. To compensate the reduced light absorption in such thin layers, extremely-thin-absorber (ETA) solar cells were proposed, in which the thin absorber is multiply folded such that the surface area of the absorber is substantially increased [3]. However, the increased surface area contributes to larger electron-hole recombination losses, decreases open circuit voltage, and, ultimately, limits conversion efficiency [4]. In order to exploit the range of earth-abundant semiconductors for solar cells, a strongly absorbing structure with a thin, planar semiconductor layer is desirable.

There have been many studies on nanostructured materials that show very high absorption in some part of the spectrum [5]–[13]. Such "perfect absorbers," in most cases, are based on absorption in a nanostructured metal and include spherical void, nanoparticle, and square patch nanoantenna geometries, among others [5]–[7]. For a solar cell, a semiconductor layer must also be included, and it is crucial that the vast majority of the absorption occurs in this layer, where it will lead to generation of electron-hole pairs, rather than in metal, where it will be lost as heat. There have been a limited number of studies where the aim has been to achieve high absorption in an ultra-thin semiconductor layer [14]–[19]. Collin *et al.* demonstrated a grating of alternating layers of

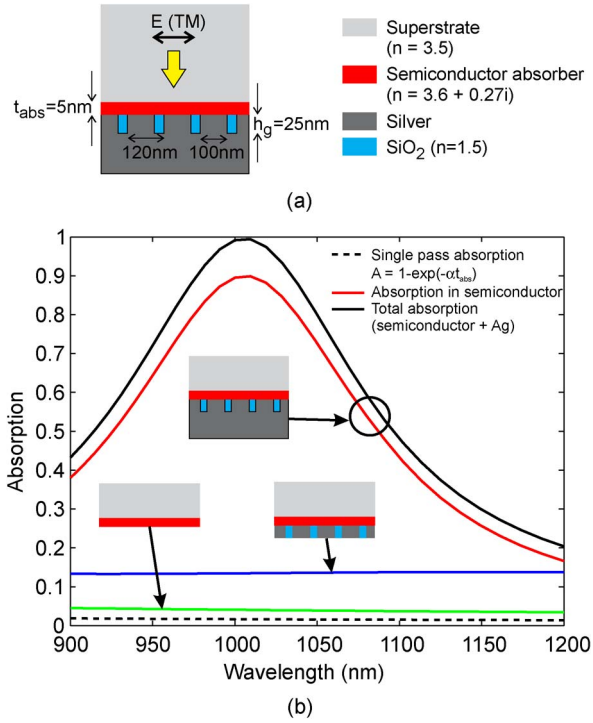


Fig. 1. (a) The modelled structure, consisting of a transparent superstrate, ultra-thin semiconductor absorber, and rear Ag/$SiO_2$ grating with Ag mirror. (b) Absorption vs. wavelength for the modelled structure, including absorption in the semiconductor (red line) and total absorption (black solid line). Also shown are the absorption in the semiconductor for single pass absorption (black dotted line), the thin semiconductor layer at the rear of a transparent superstrate (green line), and the semiconductor layer with grating but without Ag mirror (blue line).

metal and semiconductor for photodetector applications and achieved strong absorption in 40 nm GaAs wires [14]. Wang *et al.* proposed a checkerboard metallic structure sandwiching a 15 nm a-Si layer and showed that strong, broadband absorption could be achieved [15]. Core-shell geometries that can achieve strong absorption using a semiconductor shell around a metallic core have also been proposed [16].

In this paper, we propose a simple planar geometry for ultra-thin solar cell absorbers using plasmonic near-field enhancement. We use a planar structure for the semiconductor as this is expected to minimize electronic losses at the surfaces and metal on only one side of the active layer as this would simplify fabrication. We present numerical simulations showing strong broadband light absorption enhancement in an extremely thin absorber over a wide range of incident angles, with very low losses in the metal.

## 2. Simulations

The planar ultra-thin absorber geometry that we consider is shown in Fig. 1(a). It consists of a 5 nm planar absorbing layer at the rear of a semi-infinite, high index superstrate, with sub-wavelength grating formed from silicon dioxide $(SiO_2)$ and silver (Ag) grating below. Light is incident from above, and we consider only TM-polarized incident light, since TE polarization will not excite surface plasmon modes in this 1D periodic structure. We use 2D finite element simulations to investigate numerically the light reflectance and absorption in the thin absorber layer and in the metal. The material properties we consider here are based on GaAs for the superstrate and InGaAs for the absorbing layer, but we note that the plasmonic enhancement mechanism is generic, and the geometry could be readily adapted to other materials such as earth-abundant and strongly absorbing inorganic semiconductors or organic semiconductors. For this study, we consider near

infra-red wavelengths ($\lambda_0 > 900$ nm, with $\lambda_0$ being the wavelength in vacuum) where the GaAs superstrate is transparent, but the thin absorber layer has a relatively strong absorption coefficient. In order to focus on the physical mechanism of absorption enhancement, we neglect the refractive index dispersion in the semiconductor layers and use a refractive index $n = 3.5$ for the transparent superstrate. For the absorber, we use a complex refractive index $n = 3.6 + 0.27i$, which corresponds to an absorption co-efficient $\alpha = 3.39 \times 10^4$ cm$^{-1}$ at a wavelength of 1000 nm. The dispersive optical properties for silver are taken from Ref. [20].

The green line in Fig. 1(b) shows the absorption in the semiconductor absorber layer for the all-planar structure (without grating or mirror) under normal incidence. The average absorption is ~4%, much too low for an effective solar cell. The absorption is increased to ~13.6% by incorporating a periodic grating of Ag stripes with a dimension of 100 nm × 25 nm and a period of 120 nm, in direct contact with the absorbing layer, shown as the blue line in Fig. 1(b). To further increase the light absorption in the film, an Ag reflective substrate (mirror) of 100 nm thickness is put immediately below the grating, resulting in the structure shown in Fig. 1(a) and absorption in the semiconductor shown by the red curve in Fig. 1(b). The mirror is thick enough to reflect all of the light, and there is no transmission. Addition of the mirror increases the maximum absorption to 89.8% at $\lambda_0 = 1005$ nm [see Fig. 1(b)], corresponding to a 22.5 times absorption enhancement relative to the all-planar structure. This is the absorption in the 5 nm semiconductor layer only; absorption in the metal (Ag stripes and Ag mirror) remains low at ~9.6%. The total absorption in the structure is shown by the black line in Fig. 1(b), illustrating that 99.4% of the incident light is absorbed at a wavelength of ~1005 nm. The plasmonic absorption enhancement is also relatively broadband, with absorption above 50% over ~170 nm. If the high-index superstrate is removed (results not shown), the resonance blue shifts to 850 nm, and the peak absorptance in the semiconductor is reduced from about 90% to about 75%. This indicates that the superstrate assists absorption in the semiconductor and that large absorption enhancements can also be achieved without the superstrate.

The dotted black line in Fig. 1(b) shows the single pass absorption of the semiconductor film, given by $A = 1 - \exp(-\alpha t_{abs}) = 1.7\%$, where $t_{abs} = 5$ nm is the film thickness. The absorption enhancement is the ratio of the absorption in the semiconductor with the nanostructure (89.8%) to the single pass absorption, i.e., the absorption is enhanced by a factor of 53.

In our simulations, we have considered light incident from within the high-index GaAs superstrate. In a real device, the light would be incident from air, and there would be additional reflection at the air/GaAs interface. However, this could be reduced to a very low level by the use of an anti-reflection coating between the air and GaAs.

## 3. Angular and Thickness Dependence

Absorption in the semiconductor layer remains above 80% for incident angles from 0° to 80° at $\lambda_0 = 1005$ nm, as shown in Fig. 2. The angle-averaged absorption is 81.9%; 48 times higher than the single-pass absorption.

This structure does not show enhancement for TE polarized light, and the angle-averaged TE absorption is 1.3%. Even with such low TE absorption, the average absorption over all angles and both polarizations is 41.6%, which corresponds to an absorption enhancement of 28. This is well above the 2D Lambertian light-trapping enhancement limit of $\pi n$ (i.e., ~11) [18], [19]. The Lambertian value is a theoretical limit for isotropic incidence for structures that can be described using geometric optics, but higher values can be reached using wavelength-scale structures [21]–[24]. The strong enhancement shown in Fig. 1 is provided by an increased optical near-field close to the metal grating, associated with a high local density of optical states [25].

## 4. Discussion

To better understand the mechanism of the absorption enhancement, we have investigated how the optical properties of the structure change with grating depth. Fig. 3 shows the reflectance and absorptance of the full structure as a function of grating depth, showing regular sharp peaks in the

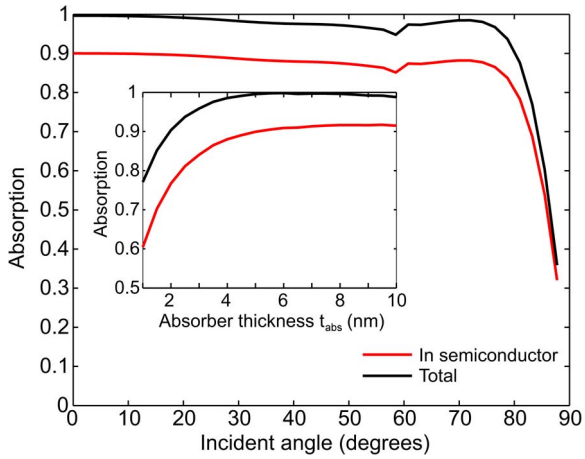


Fig. 2. Incident-angle dependence of absorption in the semiconductor (red line) and the total absorption (black line) for the structure shown in Fig. 1(a) with the Ag-stripe grating and Ag mirror. Inset: Absorption vs. thickness for the same structure under normal incidence. Both sets of data are calculated for an incident wavelength of $\lambda_0 = 1005$ nm.

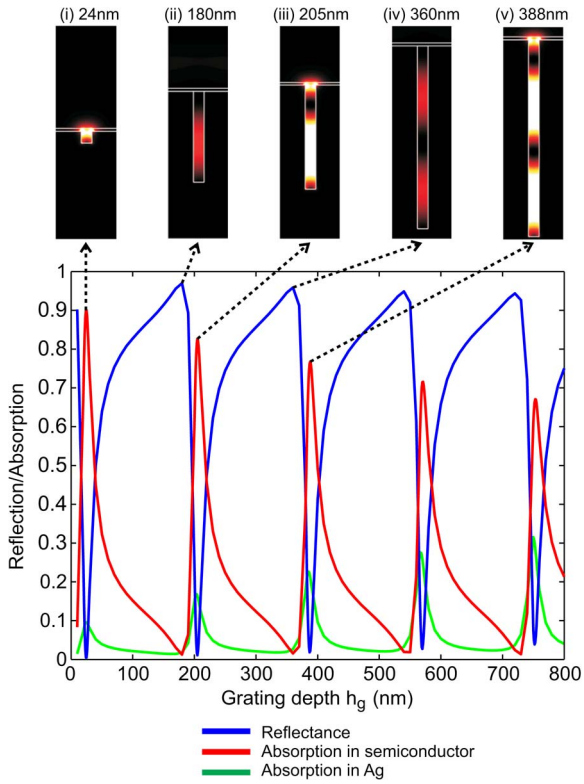


Fig. 3. Reflectance, absorptance in semiconductor layer, and absorptance within Ag vs. grating depth under normal incidence at $\lambda_0 = 1005$ nm. Also field intensity plots ($|E|^2$) at grating depths of (i) 24 nm, (ii) 180 nm, (iii) 205 nm, (iv) 360 nm, and (v) 388 nm, corresponding alternately to absorption maxima and minima.

absorptance, separated by broader peaks in the reflectance (i.e., dips in the absorptance). Also, shown in Fig. 3 are field intensity plots at grating depths corresponding to maximum and minimum absorptance in the semiconductor layer.

The field profiles and the periodic variation in the absorptance are clear evidence of a Fabry–Perot effect, with an associated high field in the InGaAs layer at certain grating depths. From the field plots, we find that the vertical spacing between nodes in the electic field profile is 180 nm. This is consistent with the spacing between the peaks in absorptance in Fig. 3. For a simple resonant cavity, the distance between the nodes is half a wavelength, i.e., from the numerical simulations, the wavelength of the propagating mode within the grooves is 360 nm.

The $SiO_2$-filled gaps between the Ag stripes can be understood as slot waveguides, or metal-insulator-metal (MIM) waveguides, which can support modes that propagate in the vertical direction. Since the incident light polarization is TM, the fundamental mode of the MIM waveguide has no cut-off. Therefore, incident light can excite a mode in the slot even when it is much narrower than the wavelength, as is the case considered here. The mode propagates to the bottom of the slot, where it is reflected by the Ag mirror. The dispersion relation for TM polarized light propagating along the $z$-direction within a MIM waveguide is given by [21], [22]

$$-\frac{k_m}{k_i} = \frac{\varepsilon_m(\omega)}{\varepsilon_i}\tanh(k_i T/2) \tag{1}$$

where $\varepsilon_m$ and $\varepsilon_i$ are the permittivities of the metal and insulator, respectively; $k_m$ and $k_i$ are the $x$-components of the wave vector in each material; and $T$ is the thickness of the insulator, in this case, the 20 nm $SiO_2$ spacer between the Ag stripes. The wave vector components

$$k_m = \sqrt{k^2 - \frac{\omega^2}{c^2}\varepsilon_m(\omega)} \quad \text{and} \quad k_i = \sqrt{k^2 - \frac{\omega^2}{c^2}\varepsilon_i(\omega)} \tag{2}$$

are defined from momentum conservation, with $k$ as the $z$-component of the wave vector. (Here, $z$ is the direction parallel to the grating grooves and normal to the semiconductor surface, while $x$ is perpendicular to the grooves and in the plane of the semiconductor surface). Note that equation (1) is for the symmetric mode, as the asymmetric mode cannot be excited by normally incident light. By solving equation (1), we find the effective wavelength of the propagating mode, i.e., $\lambda_{\text{eff}} = 2\pi/k = 363$ nm, in excellent agreement with the wavelength inferred from the numerical simulations. The high field at the top of the grooves is somewhat shifted from the position expected from the MIM model, which may be due to the change of phase at the top of the groove.

From this model, we can understand that the mirror at the rear of the grating suppresses not only the transmission of incident light but also the reflection due to destructive interference between the fields reflected from the top of the grating and the mirror. When the resonance condition for the MIM mode is satisfied, light is trapped in the cavity between the absorbing layer and the mirror until it is absorbed. At the same time, the strong field enhancement near the top surface of the grating ensures preferential absorption in the semiconductor, rather than in the metal walls of the slot. As the slot depth is increased, the light traverses a longer section of the MIM waveguide, so the relative absorption in the metal increases at each successive resonance, as seen in Fig. 3.

The strong local field enhancement at the top of the grating is not simply due to the resonance in the slot. As clearly shown in Fig. 3, there is a strong field concentration at both corners of the Ag stripes in the thin absorber layer. This near-field enhancement is associated with a localized resonant surface plasmon polariton (SPP) mode at the interface between the metal and high-index superstrate [26]. The wavelength at which the field concentration is strongest is determined by this localized plasmon resonance. We have calculated the scattering cross-section for an isolated Ag stripe of 100 nm width on the superstrate and found that the scattering resonance is centered at a wavelength of 1000 nm. The near-field enhancement is thus attributed to the interference between the Fabry–Perot like mode confined between the metal stripes and the localized plasmon mode confined at the metal-superstrate interface. The light absorption in the semiconductor thin film is therefore significantly increased, as shown in Fig. 1.

Efficient suppression of reflected light is only possible when there is a single reflected diffraction order in the superstrate, which puts an upper limit on the grating period. Based on this condition, we set the grating period to be 120 nm so that only the specular diffraction order is present in the

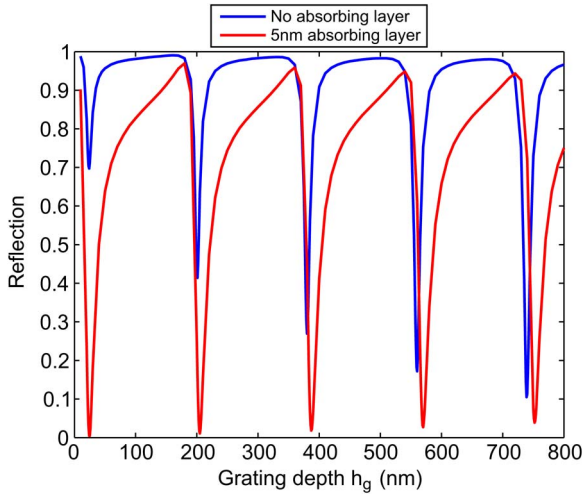


Fig. 4. Reflectance versus grating depth for the case with semiconductor absorber (red) and without absorber (blue) under normal incidence at $\lambda_0 = 1005$ nm.

superstrate for the whole studied spectrum under all the incident angles. Because only the specular diffraction order is present, the absorptance of these types of structures could also be understood by treating the grating as a metamaterial with an effective refractive index [27]. However, since the period of the grating is $\sim$1/3 of the reduced wavelength $\lambda/n$, the system is far from the homogenization limit, and an effective medium approach could only provide qualitative information for the case we study here.

Fig. 4 shows the reflectance of the structure with (red line) and without (blue line) the absorber layer. We can see that dips in the reflectance also occur when the absorber is not present, but in this case, low reflectance (strong absorptance) only occurs for large grating depths. These resonances (without an absorber layer) have also been observed by Bonod *et al.* for rectangular metal grooves [28]. A similar response was also reported by Sobnack *et al.* [29] for rounded V-shaped grooves, where the MIM mode contributing to the absorptance was identified. Sobnack *et al.* also observed that because the absorption is due to standing waves, they can be excited for a zero-order grating, which leads to flat dispersion curves and strong absorption of light for a wide range of angles. For rectangular grooves, we observe a high field near the top of the grooves. This is not seen by Sobnack *et al.*, probably because their groove is relatively wide at the top, and an MIM mode requires coupling of two plasmons propagating along metal dielectric interfaces. When the absorber layer is present, this high field near the top of the grooves occurs within the absorber, leading to the strong absorption we report here. Thus, when the absorber layer is present, strong absorption can be achieved for shallow as well as deep gratings, and in addition, the absorption occurs predominantly in the semiconductor, rather than in the metal. We also observe in Fig. 4 a slightly larger distance between the peaks for the case with absorbing layer than for the case without. We attribute this to a slight red-shift of the effective wavelength of the MIM mode, due to the high polarizability of the semiconductor absorber.

Fowler *et al.* have studied a related structure for photodetector applications [30]. In that case, they made use of a different mode of the structure, which they described as a hybrid mode, whereas here the absorption comes from a cavity mode. The semiconductor absorber thickness they considered was also much higher—100 nm compared to the 5 nm thickness we consider here.

We have demonstrated that very high absorption can be achieved in a nanometer thin layer, which has important implications for earth-abundant inorganic materials, quantum dots, and organic solar cells. In order to make a solar cell based on this optical structure, a suitable electrical design would also be required. However, this structure represents a step toward high-performance, ultra-thin solar cells from cheap materials with low electronic quality.

## 5. Conclusion

We have demonstrated a strongly absorbing ultra-thin solar cell concept based on plasmonic near-field enhancement and resonance effects. For an absorber only 5 nm thick, we calculate 89.8% maximum light absorption for normally-incident TM-polarized light, corresponding to an absorption enhancement of 53 compared with single-pass absorption. Furthermore, the enhancement is relatively broadband and angle-independent, with $>$ 50% absorption possible over a 170 nm wavelength range and over 80% light absorption for incident angles of 0° to 80°, corresponding to an absorption enhancement of 48 when averaged over all incident angles. Extending this concept to 2D periodic grating geometries is expected to provide strong angle- and polarization-independent absorption.

## Acknowledgment

The authors would like to acknowledge the Australian National University Supercomputer facility for supplying computational resources.

## References

[1] J. Poortmans and V. Arkhipov, *Thin Film Solar Cells: Fabrication, Characterization and Applications*. Hoboken, NJ, USA: Wiley, 2006.
[2] C. Wadia, A. P. Alivisatos, and D. M. Kammen, "Materials availability expands the opportunity for large-scale photovoltaics deployment," *Environ. Sci. Technol.*, vol. 43, no. 6, pp. 2072–2077, Mar. 2009.
[3] K. Ernst, A. Belaidi, and K. Könenkamp, "Solar cell with extremely thin absorber on highly structured substrate," *Semicond. Sci. Technol.*, vol. 18, no. 6, pp. 475–479, Jun. 2003.
[4] D. Kieven, T. Dittrich, A. Belaidi, J. Tornow, K. Schwarzburg, N. Allsop, and M. Lux-Steiner, "Effect of internal surface area on the performance of ZnO/$In_2S_3$/CuSCN solar cells with extremely thin absorber," *Appl. Phys. Lett.*, vol. 92, no. 15, pp. 153107-1–153107-3, Apr. 2008.
[5] T. V. Teperik, F. J. García de Abajo, A. G. Borisov, M. Abdelsalam, P. N. Bartlett, Y. Sugawara, and J. J. Baumberg, "Omnidirectional absorption in nanostructured metal surfaces," *Nat. Photon.*, vol. 2, no. 5, pp. 299–301, May 2008.
[6] V. G. Kravets, S. Neubeck, and a. N. Grigorenko, "Plasmonic blackbody: Strong absorption of light by metal nanoparticles embedded in a dielectric matrix," *Phys. Rev. B, Condens. Matter*, vol. 81, no. 16, pp. 165401-1–165401-9, Apr. 2010.
[7] P. Bouchon, C. Koechlin, F. Pardo, R. Haïdar, and J.-L. Pelouard, "Wideband omnidirectional infrared absorber with a patchwork of plasmonic nanoantennas," *Opt. Lett.*, vol. 37, no. 6, pp. 1038–1040, Mar. 2012.
[8] J. Le Perchec, P. Quémerais, A. Barbara, and T. López-Ríos, "Why metallic surfaces with grooves a few nanometers deep and wide may strongly absorb visible light," *Phys. Rev. Lett.*, vol. 100, no. 6, pp. 066408-1–066408-4, Feb. 2008.
[9] E. Popov, D. Maystre, R. C. McPhedran, M. Nevière, M. C. Hutley, and G. H. Derrick, "Total absorption of unpolarized light by crossed gratings," *Opti. Exp.*, vol. 16, no. 9, pp. 6146–6155, Apr. 2008.
[10] S. Thongrattanasiri, F. Koppens, and F. García de Abajo, "Complete optical absorption in periodically patterned graphene," *Phys. Rev. Lett.*, vol. 108, no. 4, pp. 047401-1–047401-5, Jan. 2012.
[11] J. Hao, L. Zhou, and M. Qiu, "Nearly total absorption of light and heat generation by plasmonic metamaterials," *Phys. Rev. B, Condens. Matter*, vol. 83, no. 16, pp. 165107-1–165107-12, Apr. 2011.
[12] K. Aydin, V. E. Ferry, R. M. Briggs, and H. A Atwater, "Broadband polarization-independent resonant light absorption using ultrathin plasmonic super absorbers," *Nat. Commun.*, vol. 2, no. 10, p. 517, Nov. 2011.
[13] P. Zhu and L. Jay Guo, "High performance broadband absorber in the visible band by engineered dispersion and geometry of a metal-dielectric-metal stack," *Appl. Phys. Lett.*, vol. 101, no. 24, pp. 241116-1–241116-4, Dec. 2012.
[14] S. Collin, F. Pardo, R. Teissier, and J.-L. Pelouard, "Efficient light absorption in metal–semiconductor–metal nanostructures," *Appl. Phys. Lett.*, vol. 85, no. 2, pp. 194–196, Jul. 2004.
[15] Y. Wang, T. Sun, T. Paudel, Y. Zhang, Z. Ren, and K. Kempa, "Metamaterial-plasmonic absorber structure for high efficiency amorphous silicon solar cells," *Nano Lett.*, vol. 12, no. 1, pp. 440–445, Jan. 2012.
[16] C. Hagglund and S. P. Apell, "Plasmonic near-field absorbers for ultrathin solar cells," *J. Phys. Chem. Lett.*, vol. 3, no. 10, pp. 1275–1285, May 2012.
[17] R. A. Pala, J. White, E. Barnard, J. Liu, and M. L. Brongersma, "Design of plasmonic thin-film solar cells with broadband absorption enhancements," *Adv. Mater.*, vol. 21, no. 34, pp. 3504–3509, Sep. 2009.
[18] J. N. Munday and H. a Atwater, "Large integrated absorption enhancement in plasmonic solar cells by combining metallic gratings and antireflection coatings," *Nano Lett.*, vol. 11, no. 6, pp. 2195–2201, Jun. 2011.
[19] X. Sheng, J. Hu, J. Michel, and L. C. Kimerling, "Light trapping limits in plasmonic solar cells: An analytical investigation," *Opt. Exp.*, vol. 20, no. S4, pp. 496–501, Jul. 2012.
[20] P. B. Johnson and R. W. Christy, "Optical constants of the noble metals," *Phys. Rev. B, Condens. Matter*, vol. 6, no. 12, pp. 4370–4379, Dec. 1972.
[21] Z. Yu, A. Raman, and S. Fan, "Fundamental limit of nanophotonic light trapping in solar cells," *Proc. Nat. Acad. Sci. USA*, vol. 107, no. 41, pp. 17 491–17 496, Sep. 2010.

[22] M. A. Green, "Enhanced evanescent mode light trapping in organic solar cells and other low index optoelectronic devices," *Progr. Photovolt.*, vol. 19, no. 4, pp. 473–477, Jun. 2011.
[23] E. A. Schiff, "Thermodynamic limit to photonic-plasmonic light-trapping in thin films on metals," *J. Appl. Phys.*, vol. 110, no. 10, pp. 104501-1–104501-9, Nov. 2011.
[24] J. N. Munday, D. M. Callahan, and H. a. Atwater, "Light trapping beyond the$4n_2$ limit in thin waveguides," *Appl. Phys. Lett.*, vol. 100, no. 12, pp. 121121-1–121121-4, Mar. 2012.
[25] D. M. Callahan, J. N. Munday, and H. A. Atwater, "Solar cell light trapping beyond the ray optic limit," *Nano Lett.*, vol. 12, no. 1, pp. 214–218, Jan. 2011.
[26] F. J. Beck, E. Verhagen, S. Mokkapati, A. Polman, and K. R. Catchpole, "Resonant SPP modes supported by discrete metal nanoparticles on high-index substrates," *Opt. Exp.*, vol. 19, no. S2, pp. A146–A156, Mar. 2011.
[27] E. Popov, S. Enoch, and N. Bonod, "Absorption of light by extremely shallow metallic gratings: Metamaterial behavior," *Opt. Exp.*, vol. 17, no. 8, pp. 6770–6781, Apr. 2009.
[28] N. Bonod, G. Tayeb, D. Maystre, S. Enoch, and E. Popov, "Total absorption of light by lamellar metallic gratings," *Opt. Exp.*, vol. 16, no. 20, pp. 15 431–15 438, Sep. 2008.
[29] M. B. Sobnack, W. C. Tan, N. P. Wanstall, T. W. Preist, and J. R. Sambles, "Stationary surface plasmons on a zero-order metal grating," *Phys. Rev. Lett.*, vol. 80, no. 25, pp. 5667–5670, Jun. 1998.
[30] D. Fowler, S. Boutami, M. Duperron, G. Moille, G. Badano, F. Boulard, J. Rothman, O. Gravrand, and R. Espiau de Lamaestre, "Partially localized hybrid surface plasmon mode for thin-film semiconductor infrared photodetection," *Opt. Lett.*, vol. 38, no. 3, pp. 254–256, Feb. 2013.